CHEMISTRY OF MATERIALS

ARTICLE

pubs.acs.org/cm

Degradable and Electroactive Hydrogels with Tunable Electrical Conductivity and Swelling Behavior

Baolin Guo, Anna Finne-Wistrand, and Ann-Christine Albertsson*

Department of Fibre and Polymer Technology, School of Chemical Science and Engineering, Royal Institute of Technology, SE-100 44, Stockholm, Sweden

Supporting Information

ABSTRACT: Degradable electrically conducting hydrogels (DECHs), which combine the unique properties of degradable polymers and electrically conducting hydrogels, were synthesized by introducing biodegradable segments into conductive hydrogels. These DECHs were obtained by joining together the photopolymerized macromer acrylated poly(D,L-lactide)−poly(ethylene glycol)−poly(D,L-lactide) (AC-PLA-PEG-PLA-AC), glycidyl methacrylate (GMA), ethylene glycol dimethacrylate (EGDMA) network and aniline tetramer (AT) by the coupling reaction between AT and the GMA. The electrical conductivity and swelling behavior of these DECHs were tuned by changing the AT content in the hydrogels, the cross-linking degree, and the environmental pH value. The good electroactivity and thermal stability of these hydrogels were demonstrated by UV−vis spectroscopy, cyclic voltammetry, and TGA tests. The chemical structure and morphology of these polymers were characterized by NMR, FT-IR, SEC, and SEM. These hydrogels possessing both degradability and electrical conductivity represent a new class of biomaterial and will lead to various new possibilities in biomedical applications.

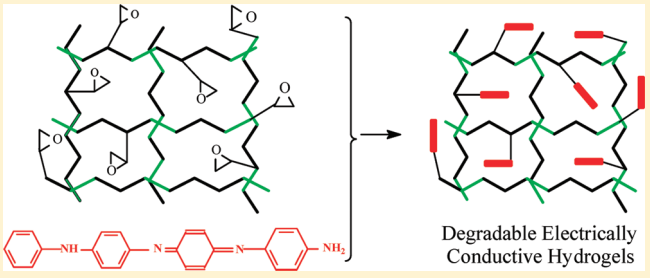

KEYWORDS: degradable and conductive hydrogels, electroactive and biodegradable polymers, conductive polymers, tissue engineering

INTRODUCTION

The third-generation biomaterials, once implanted, will help the body heal itself and are designed to induce specific cellular responses at the molecular level.[1] Third-generation biomaterials combine the separate concepts of bioactive materials and resorbable materials. Recent studies have demonstrated that electrical stimuli can adjust a range of cellular activities, such as cell adhesion, migration, and proliferation.[2−5] Inherently electrically conductive polymers such as polyaniline and polypyrrole are widely used in the biomedical field,[6−8] but they are not degradable. The degradable electrically conducting polymers (DECPs) possessing both electrical conductivity and degradability are therefore attracting great attention.[9−13] For instance, erodible conducting polymers consisting of β-substituted pyrrole monomers with ionizable and/or hydrolyzable side groups were synthesized by Langer et al.[9] Schmidt et al.[10] connected conducting oligomers of pyrrole and thiophenes by degradable ester linkages, and the copolymers showed good conductivity, degradability, and biocompatibility. We have synthesized star-shaped[12] and hyperbranched[13] copolymers composed of polylactide, polycaprolactone, and aniline oligomers, carboxyl-capped aniline trimer, and aniline pentamer, which are electroactive and degradable. We found that macromolecular architecture is a useful tool to enhance the conductivity of the polymers. These copolymers also exhibit better solubility, greater hydrophilicity, and better processability than polyaniline and polypyrrole. However, the synthesis of DECPs remains a challenge. There are linear, star-shaped, and hyperbranched architecture of DECPs, but so far no cross-linked network of DECPs has been reported.

Hydrogels, three-dimensional cross-linked hydrophilic polymer networks, represent an important class of biomaterials, because of their rubbery nature similar to soft tissues, their easy control of oxygen, nutrients, and other bioactive molecules, and their excellent biocompatibility as reviewed by Lee and Mooney[14] and Langer et al.[15] During the past couple of decades, hydrogels have attracted much attention; many hydrogels with different structures, compositions, and properties have been designed and fabricated, and they are widely used in the biomedical field. Our group has synthesized a series of biodegradable hydrogels from functional aliphatic polyesters and renewable resources.[16−19] One of the recent trends in hydrogel synthesis is to use photopolymerization[20−23] or phase transition[24,25] to form in situ hydrogels. Photopolymerization reactions maintain good spatial and temporal control over the gelation reaction and can be carried out under ambient or physiological conditions.[18,19,26,27] Photopolymerized hydrogels have already been used for biomedical applications such as drug delivery[28,29] and cell transplantation.[30,31]

Received: October 29, 2010
Published: January 12, 2011

Electrically conducting hydrogels (ECHs) which are polymeric blends or co-network biomaterials have been developed recently by Guiseppi-Elie and Wilson[32,33] and Wallace et al.[34] ECHs combined the unique advantages of redox, optical switching, and electrical properties of inherently conducting polymers, the facile diffusivity of small molecules, and high degree of hydration and good biocompatibility of hydrogels. ECHs originating from the inherent properties of the constituent components possess the biologically relevant properties for devices.[33,35−37] For example, polypyrrole/poly(styrene sulfonate sodium salt) could be used as an effective ion-exchange material for the ON−OFF switching release of biologically relevant cations.[38,39] Conducting electroactive hydrogels composed of 2-hydroxy ethyl methacrylate and polypyrrole were synthesized, and these hydrogels, by the introduction of analyte-specific enzymes, had a potential application as biomedical diagnostic biosensors.[40] However, none of the reported electrically conducting hydrogels is degradable, which severely limits their application in the biomedical field where degradation is desirable or even necessary in more advanced tissue engineering application.

On the basis of early experience of DECPs[12,13] and degradable (hydro)gels,[16−19] our objective was thus to develop the complete degradable electrically conducting hydrogels (DECHs) by introducing biodegradation properties into the electrically conducting hydrogels. We hypothesize that DECHs combining the advantages of degradable electrically conducting polymers and the unique properties of hydrogels will open a novel exciting area of third generation biomaterials. We designed and synthesized the first example of DECH, AC-PLA-PEG-PLA-AC/GMA/AT, and these DECHs have tunable electrical conductivity and a controlled hydration percentage. These DECHs were synthesized by a two-step reaction. First, we used photopolymerization to obtain a degradable network of the macromer AC-PLA-PEG-PLA-AC/EGDMA/GMA to introduce the epoxy group into the network, and the well-defined structured aniline tetramer (AT) monomer was then covalently linked to the network by the coupling reaction between the amino group of AT and the epoxy group in GMA. The electrical conductivity and hydration percentage of the obtained hydrogels were tuned by the AT content, cross-linking degree, and surrounding pH, which provide a wide range of choice for any specific biomedical application, such as controlled drug delivery systems, neural, bone, muscle, ear, and cardiovascular tissue regeneration.

EXPERIMENTAL SECTION

Materials. D,L-Lactide was recrystallized in dry toluene and subsequently dried under reduced pressure (10^{-2} mbar) at room temperature for at least two days before polymerization. Toluene (Lab-Scan, 99.8%) was dried over a Na wire before use. Stannous octoate, $Sn(Oct)_2$ (Sigma-Aldrich, Sweden) was dried over molecular sieves prior to use. Glycidyl methacrylate (GMA), ethylene glycol dimethacrylate (EGDMA), polyethylene glycol 6000 (PEG6000), acryloyl chloride (AC), triethylamine, dichloromethane, photoinitiator 2,2-dimethoxy-2-phenylacetophenone (DMPA), *N*-phenyl-1,4-phenylenediamine, ammonium persulphate ($(NH_4)_2S_2O_8$), ammonium hydroxide (NH_3OH), hydrochloric acid (HCl), dimethyl sulphoxide (DMSO), diethyl ether, chloroform ($CHCl_3$), and tetrahydrofuran (THF) were all purchased from Aldrich and were used without further purification.

Synthesis of Aniline Tetramer (AT). AT was synthesized according to refs 41 and 42. Briefly, *N*-phenyl-1,4-phenylenediamine was oxidized by equivalent amounts of $(NH_4)_2S_2O_8$ in an acetone/1 mol/L HCl mixture, as shown in Scheme 1. The NMR spectrum of AT is shown in Figure 1. ^{1}H NMR (400 MHz, DMSO-d_6): 8.38 (s, 1H), 7.24 (t, 2H), 7.09 (s, 4H), 7.03−6.96 (m, 5H), 6.91−6.80 (m, 2H), 6.82−6.79 (m, 2H), 6.61−6.60 (m, 2H), 5.53 (s, 2H). These results agree well with data in the literature.[41] There is only one peak at 5.53 ppm, and no peak at 4.69 ppm, indicating that only one isomer as shown in Scheme 1 exists in the DMSO solution.[41]

Synthesis of AC-PLA-PEG-PLA-AC Macromonomer. Macromonomer AC-PLA-PEG-PLA-AC was synthesized as described in a previous publication.[43] Briefly, the PLA-PEG-PLA copolymer was obtained by a ring-opening polymerization with D,L-lactide (1 g) initiated by PEG6000 (3 g) and $Sn(Oct)_2$ (8 mg) as a catalyst at 110 °C for 48 h. The purified PLA-PEG-PLA copolymer was then acrylated by acryloyl chloride with triethylamine as the catalyst in dichloromethane. The AC-PLA-PEG-PLA-AC was then precipitated in cold ether and filtered. The AC-PLA-PEG-PLA-AC was dissolved in $CHCl_3$, and the triethylamine was then extracted three times in deionized water and precipitated in ether. After filtration, the AC-PLA-PEG-PLA-AC was dried in a vacuum oven for 48 h.

Synthesis of Degradable AC-PLA-PEG-PLA-AC/GMA Hydrogels by Photopolymerization. Appropriate amounts (see Table 1) of macromer AC-PLA-PEG-PLA-AC, GMA, EGDMA, photoinitiator DMPA (1.5 wt % of all the monomers), and THF as solvent were weighed and transferred to a small vial. The solution was then placed under UV-lamp. The distance between the vials and lamp was about 20 cm. Photopolymerization was subsequently conducted using an Osram Ultra-Vitalux 300-W lamp which provided homogeneous solar-like illumination with an irradiation intensity of 80 mW/cm^2. The reaction was maintained for 1 h as shown in Scheme 1. The cross-linked network was obtained after evaporation of THF. The hydrogel was then placed in distilled water for 2 days to remove the unreacted monomer, the water being changed from time to time.

Synthesis of Degradable and Conductive AC-PLA-PEG-PLA-AC/GMA/AT Hydrogels. Different amounts of AT as shown in Table 1 were added to the above solution before evaporation of THF. The coupling reaction between the amino group of AT and the epoxy group of GMA was carried out at 50 °C for 12 h.[44,45] After the reaction, the THF was evaporated at room temperature. The hydrogel was immersed in a water/THF mixture to remove unreacted AT and monomers. Finally the hydrogels were dried in a vacuum oven for 3 days. The synthetic route is shown in Scheme 1.

The degradable conductive hydrogels with different degrees of cross-linking were synthesized by adding different amounts of EGDMA to the system with the AT content of 20 wt %. These samples were coded as 5% EGDMA hydrogel, 10% EGDMA hydrogel, 20% EGDMA hydrogel, and 30% EGDMA hydrogel, respectively, which means that the EGDMA amounts were 5%, 10%, 20%, and 30% by weight of the macromer AC-PLA-PEG-PLA-AC.

Characterization. FT-IR spectra of the AC-PLA-PEG-PLA-AC/GMA mixture, the AC-PLA-PEG-PLA-AC/GMA solution after UV photo-cross-linking, and the AT and the AT-coupled AC-PLA-PEG-PLA-AC/GMA hydrogel (AC-PLA-PEG-PLA-AC/GMA/AT) were recorded using a Perkin Elmer Spectrum 2000 spectrometer (Perkin-Elmer Instrument, Inc.) in the range of 4000−600 cm^{-1}. Each spectrum was taken as the average of 16 scans at a resolution of 4 cm^{-1}.

^{1}H NMR (400 MHz) and ^{13}C NMR (100 MHz) spectra were obtained using a Bruker Avance 400 MHz NMR instrument with $CDCl_3$ as the solvent at room temperature for the PLA-PEG-PLA and AC-PLA-PEG-PLA-AC samples and internal standard (δ = 7.26 and 77.0 ppm) and DMSO-d_6 as solvent for the AT sample and internal standard (δ = 2.50 ppm).

Molecular weights of the macromonomer PLA-PEG-PLA and AC-PLA-PEG-PLA-AC were determined by size exclusion chromatography (SEC) using a TDA Model 301 equipped with one or two GMH_{HR}-M columns with TSK-gel (Tosoh Biosep), a VE 5200 GPC Autosampler, a

Scheme 1. Schematic Synthesis of the Degradable and Electroactive Hydrogels

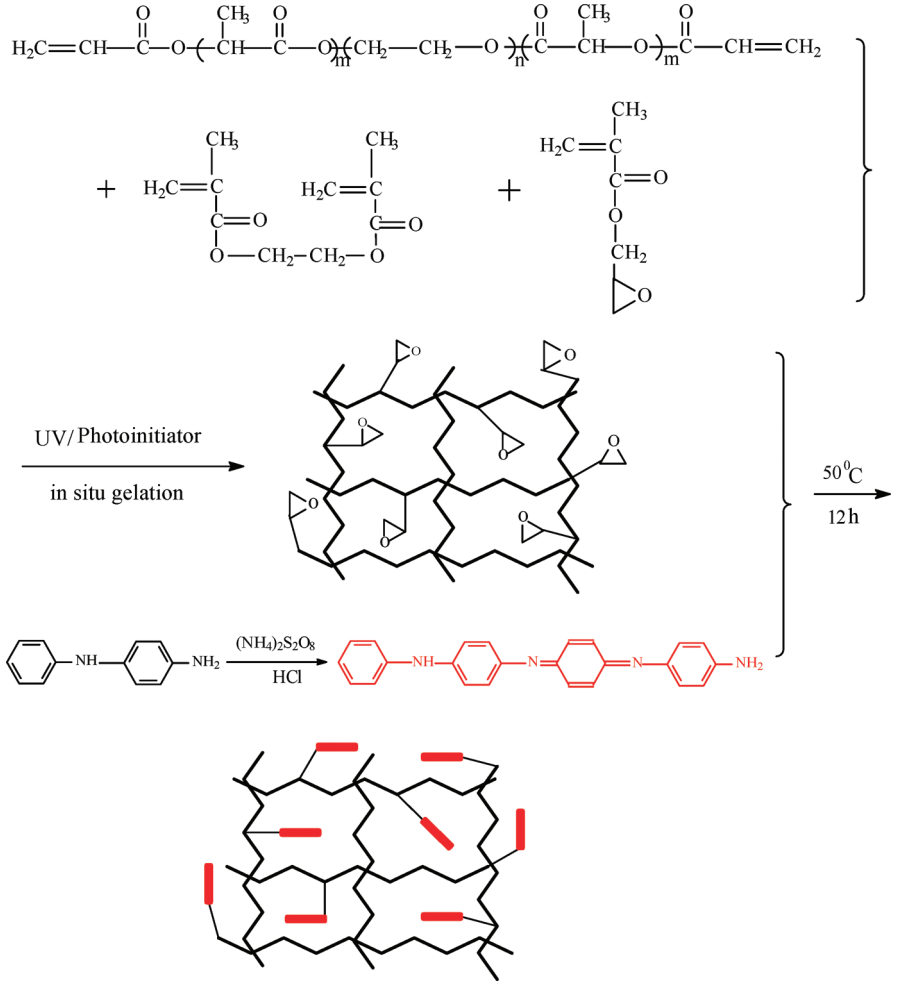

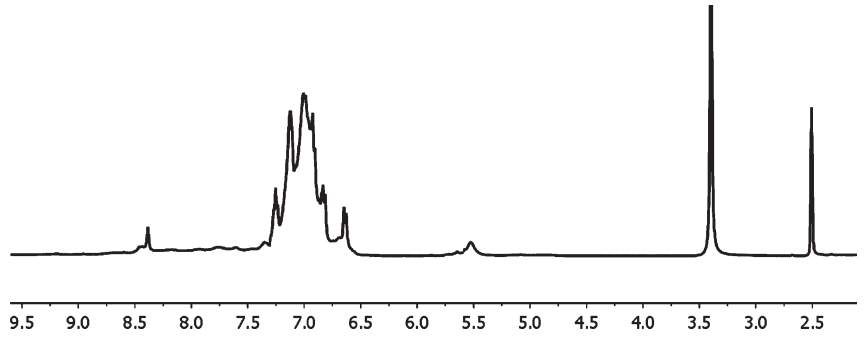

Figure 1. ^{1}H NMR of aniline tetramer in DMSO-d_6.

VE 1121 GPC Solvent pump and a VE 5710 GPC Degasser, all of which were from Viscotek Corp. THF was used as the mobile phase (flow rate 1.0 mL/min), and the test was carried out at 35 °C. The SEC apparatus was equipped with a differential refractive index detector and differential viscometer. A linear polystyrene standard was used to calibrate the SEC apparatus.

The UV−vis spectra of AT, the AC-PLA-PEG-PLA-AC/GMA/AT hydrogel, and their corresponding HCl-doped solutions were recorded with a UV−vis spectrophotometer (UV-2401).

The hydration percentage (HP) of the hydrogels was determined by immersing the dry hydrogels in aqueous solutions of the desired pH in sealed containers. The hydrogels were removed from the aqueous solution after regular periods of time, weighed, and returned to the same container after the removal of excess surface water with filter paper, until swelling equilibrium was reached. HP is calculated as HP = $[(W_s - W_d)/W_d] \times 100\%$, while sol fraction is determined by sol fraction = $[(W_i - W_d)/W_d] \times 100\%$, where W_i, W_s, and W_d are the weight of dried hydrogel after cross-linking, the weight of hydrogel

dx.doi.org/10.1021/cm103498s |*Chem. Mater.* 2011, 23, 1254–1262

Table 1. Feed Compositions of the Hydrogels with Different AT Contents

components	sample name: 10% AT hydrogel	20% AT hydrogel	30% AT hydrogel	40% AT hydrogel
m(AC-PLA-PEG-PLA-AC) (mg)	400	400	400	400
m(EGDMA) (mg)	40	40	40	40
m(GMA) (mg)	21	47	90	156
m(DMPA) (mg)	9.2	9.7	10.6	11.9
m(AT) (mg)	52	120	230	400

at swollen state, and the weight of the dried hydrogels after swelling, respectively.

Thermogravimetric analysis (TGA) of the hydrogel samples was used to determine the AT content and the thermal stability of the hydrogels. The TGA test was carried out with a heating rate of 10 °C/min from 30 to 800 °C under a nitrogen atmosphere (nitrogen flow rate 50 mL/min).

The morphology of the hydrogels mounted on metal stubs was examined using a field emission scanning electron microscope (FE-SEM, S-4300, Hitachi, Japan).

Cyclic voltammetry (CV) of AT and a highly swollen 5% EGDMA hydrogel solution was conducted on an Electrochemical Workstation employing a three-electrode system with a platinum disk as working electrode (surface area 0.14 cm^2), a platinum wire as auxiliary electrode, and an Ag/AgCl as reference electrode. The scan rate was 60 mV/s for all the samples. The AT monomer and hydrogel samples were dissolved or swelled in a DMSO for 24 h. The solutions were doped with 1 mol/L HCl and were then deoxygenated for 10 min with nitrogen prior to the electrochemical measurements. The electrical conductivity of the 1 mol/L HCl doped hydrogel pellets dried in a vacuum oven was determined by the standard Van Der Pauw four-probe method.[46,47] The compressed pellets with a diameter of 2.0 cm and a thickness of 0.045 cm were made in a compression mold equipment at 40 °C with a pressure of 50 KN/m^2. The conductivity of each sample was determined four times at different current values, and the average value was taken as the conductivity of the sample.

RESULTS AND DISCUSSION

Synthesis of the AC-PLA-PEG-PLA-AC Macromonomer. Hydrogels obtained from the photopolymerization of macromolecular monomers are an important kind of biomaterial that are increasingly being applied as in situ materials for cell encapsulation and tissue regeneration.[48,49] The AC-PLA-PEG-PLA-AC has good hydrophilicity, biocompatibility, and biodegradability. The ^1H and ^{13}C NMR spectra of AC-PLA-PEG-PLA-AC are shown in Supporting Information. ^1H NMR (400 MHz, $CDCl_3$) δ = 6.40−6.44 (d, 2H, CH_2═C—COO— (trans)), δ = 6.09−6.16 (d, 1H, —C═CH—COO), δ = 5.84−5.86 (d, 2H, CH_2═C—COO— (cis)), δ = 5.14 (m, H, —CH—), δ = 4.24 (t, 2H, —CH_2—), δ = 3.59 (s, 2H, —CH_2—O), δ = 1.52 (d, 3H, —CH_3). ^{13}C NMR (100 MHz, $CDCl_3$) δ = 169.5 (—CO—), δ = 165.3 (—OOC—CH_2═C—), δ = 131.9 (CH_2═CH—), δ = 127.5 (—CH_2═CH—), δ = 70.5 (—CH_2—CH_2—O), δ = 68.7 (—CH—), δ = 64.4 (—CH_2—), δ = 16.7 (—CH_3). The presence of the peak at 4.24 ppm corresponding to the methylene proton of PEG6000 at the linkage between PEG and PLA demonstrates the formation of PLA-PEG-PLA block copolymer. The average number of LA units in the PLA blocks was determined by comparing the integral of the peak at 5.14 ppm assigned to the −CH− group of PLA with that of the peak at 3.59 ppm corresponding to the −CH_2− group of PEG segment, and the value is 8. Thus, the molecular weight of the PLA-PEG-PLA copolymer calculated by NMR was 7075. This is very close to the molecular weight of 7200 obtained from SEC. The polymer PLA-PEG-PLA also has a narrow molecular weight distribution of about 1.27. In the case of the AC-PLA-PEG-PLA-AC macromer, the three peaks between 6.09 ppm and 5.84 ppm (see Supporting Information), which are assigned to the protons of the acrylate, confirmed the successful acrylation reaction between the PLA-PEG-PLA and the acryloyl chloride. This reaction was also confirmed by the ^{13}C NMR spectrum of AC-PLA-PEG-PLA-AC, in which two new peaks at 131.9 ppm and 127.5 ppm are ascribed to the unsaturated carbon. The percentage of acrylation of AC-PLA-PEG-PLA-AC was calculated by comparing the integral of peak at 4.25 ppm corresponding to the −CH_2− chain end of PEG with that of peaks at 5.84−6.44 ppm assigned to the double bond. The AC-PLA-PEG-PLA-AC has a quite high acrylation percentage which is 98%. The molecular weight of AC-PLA-PEG-PLA-AC determined by SEC was 7800, and polydispersity was 1.21. All these data show the successful synthesis of the macromonomer AC-PLA-PEG-PLA-AC.

Synthesis of DECHs. Since AT is a free radical inhibitor,[50] using free radical polymerization to incorporate AT into polymers does not work without the protection of the −NH− groups in AT by tert-butoxycarbonyl groups,[51] and it needs to deprotect the tert-butoxycarbonyl group in the polymer by heating to about 200 °C or by acid catalyzed hydrolysis, which is not suitable for biomaterials. We first introduced GMA with its epoxy group into the network, and the AT segments were then chemically linked to the network by the coupling reaction between the amino group in AT and the epoxy group in GMA for the synthesis of DECHs. The AT segments during the degradation of the hydrogels would be consumed by macrophages, reducing the long-term adverse response.[10] By changing the AT content and the EGDMA content in the network, we obtained a series of AC-PLA-PEG-PLA-AC/GMA/AT hydrogels with different conductivities and different HPs. FT-IR was used to trace the formation of these DECHs. The FT-IR spectra of the macromer AC-PLA-PEG-PLA-AC/GMA mixture, the AC-PLA-PEG-PLA-AC/GMA mixture after UV irradiation, and the AT and the AC-PLA-PEG-PLA-AC/GMA/AT hydrogel are shown in Figure 2 as curves a, b, c, and d, respectively. The peak at 1636 cm^{-1} corresponding to the double bonds (C═C) in the AC-PLA-PEG-PLA-AC/GMA mixture is clearly seen in curve a. However, such a peak was absent in curve b after the UV irradiation for 60 min, indicating that photopolymerization had taken place between the AC-PLA-PEG-PLA-AC, GMA, and EGDMA. At the same time, a new peak at 909 cm^{-1} which is assigned to the epoxy group in the GMA is evident in curve b. The peak of the epoxy group disappeared completely in curve d, while new peaks at 1597 cm^{-1} and 1495 cm^{-1} corresponding to the benzene ring and the quinoid ring in AT appeared. Furthermore, the characteristic absorbance peaks at 3367 cm^{-1} and 3192 cm^{-1} of the amine −NH_2 group in AT in curve c changed into a single peak at 3320 cm^{-1} in curve d, due to the formation of the imine −NH−, indicating that the coupling reactions between the epoxy group and the amino group of AT had occurred. The AT segments were thus successfully covalently linked to the AC-PLA-PEG-PLA-AC/GMA network. All these results demonstrated that the AC-PLA-PEG-PLA-AC/GMA/AT hydrogels were successfully synthesized.

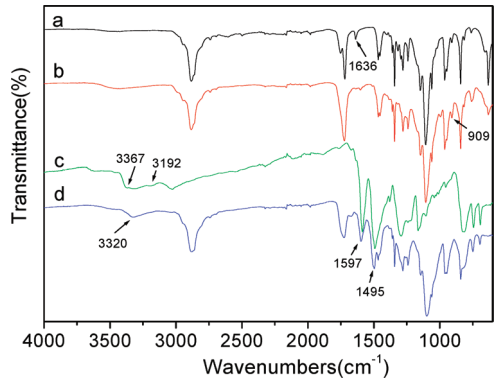

Figure 2. FT-IR spectra of (a) macromer AC-PLA-PEG-PLA-AC/GMA mixture, (b) AC-PLA-PEG-PLA-AC/GMA mixture after UV irradiation, (c) aniline tetramer, and (d) AC-PLA-PEG-PLA-AC/GMA/AT hydrogel.

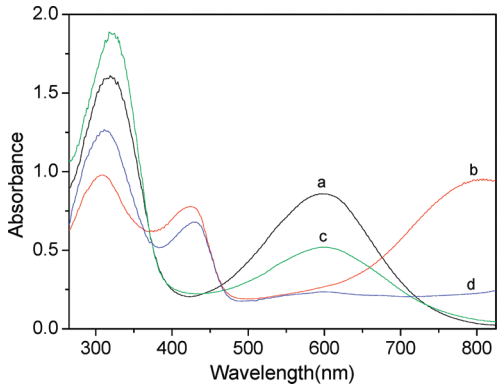

Figure 3. UV spectra of (a) AT, (b) HCl-doped AT, (c) 5% EGDMA hydrogel, and (d) HCl-doped 5% EGDMA hydrogel in DMSO solution.

Electrochemical Properties of Hydrogels. The electrochemical properties of the monomer and of the hydrogels were investigated by UV spectrometry and cyclic voltammetry. DMSO is a good solvent for all the components of the hydrogel. 5% EGDMA hydrogel with a very low cross-linking density can swell considerably and partially dissolve in DMSO, and this makes it possible to study the electrochemical properties of these hydrogels. The UV spectra of (a) AT, (b) HCl-doped AT, (c) 5% EGDMA hydrogel, and (d) HCl-doped 5% EGDMA hydrogel are shown in Figure 3. The UV spectra of both AT and 5% EGDMA hydrogel show two absorbance peaks at about 318 and 600 nm, which are ascribed to the $\pi-\pi^*$ transition of the benzene ring and the benzenoid (B) to quinoid (Q) $\pi_B-\pi_Q$ excitonic transition.[52] Obviously, compared with the Q/B intensity ratio of AT, the ratio of the 5% EGDMA hydrogel decreased dramatically together with a slight blue shift, which is probably because the $-NH-CH_2-$ group is an electron-withdrawing group compared to $-NH_2$, which reduces the electronic concentration of the quinone units, and this also confirmed that the coupling reaction between the amino group and epoxy group had occurred. When AT was doped with HCl solution, two new absorption peaks appeared at 426 and 797 nm, and there was a slight blue shift of the benzenoid absorption peak to 309 nm due to the formation of delocalized polarons; however, the UV spectrum of doped 5% EGDMA hydrogel showed only one new

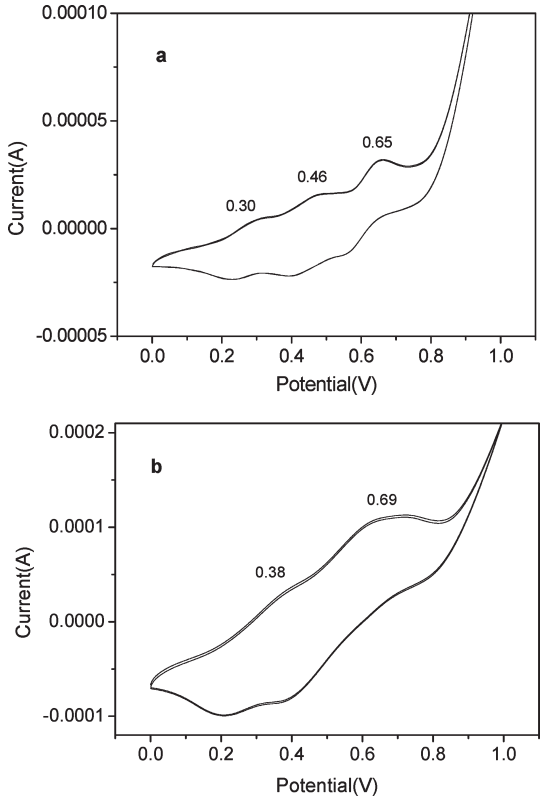

Figure 4. Cyclic voltammograms of (a) AT and (b) 5% EGDMA hydrogel in DMSO solution doped with 1 mol/L HCl, scan rate 60 mV/s.

Scheme 2. Molecular Structure of AT Monomer in Various Oxidation and Isomer States

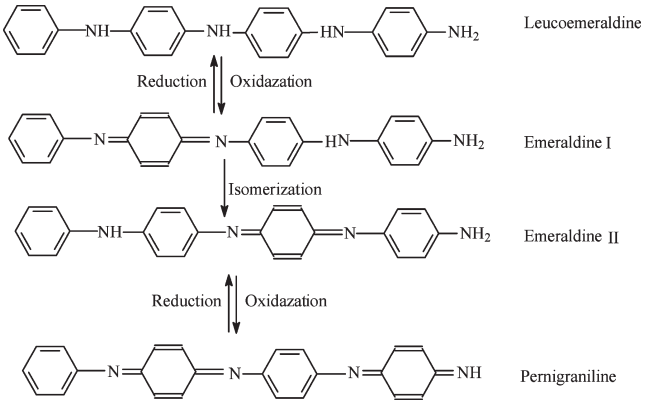

peak at 429 nm compared to that of AT, which is also probably due to the formation of a positive induction group $-NH-CH_2-$ from the coupling reaction between the amino group $-NH_2$ of AT and the epoxy group in the hydrogel network.

Figure 4 shows the cyclic voltammograms of (a) the monomer AT and (b) the 5% EGDMA hydrogel. In Figure 4a, there are three pairs of oxidation/reduction peaks at 0.30 V, 0.46 V, and 0.65 V for AT, and the proposed mechanism of the changes of molecular structure are shown in Scheme 2. The first two peaks at 0.30 and 0.46 V are assigned to the transition from the leucoemeraldine base state to the emeraldine I and emeraldine II states. The emeraldine I state will transform into the emeraldine

Scheme 3. Molecular Structure of AT Segments in 5% EGDMA Hydrogel in Various Oxidation States

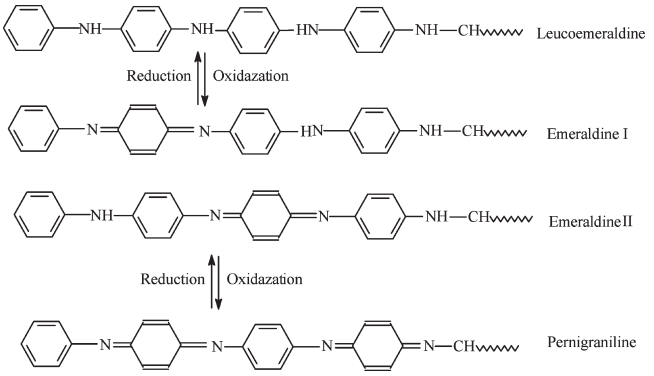

II state by isomerization, since only the emeraldine II state exists in the DMSO solution, as indicated by the ^{1}H NMR spectrum of AT in Figure 1. The third oxidation peak at 0.65 V corresponds to the transition from the emeraldine II state to the pernigraniline state (Scheme 2). However, the cyclic voltammogram of the 5% EGDMA hydrogel exhibited two oxidation peaks at 0.38 and 0.69 V, which are probably ascribed to the transition from the leucoemeraldine base state to the emeraldine I or emeraldine II states and from the emeraldine I or emeraldine II state to the pernigraniline state, as shown in Scheme 3. The higher oxidation potential of the hydrogel, 0.69 V, compared to the 0.65 V of AT could also be due to the positive induction effect of the $-NH-CH_2-$ group compared to the $-NH_2$ group, which stabilizes the AT segments in the hydrogel and increases the oxidation energy barrier between the emeraldine state to the pernigraniline state. We speculate that when the leucoemeraldine base was oxidized to the emeraldine state, only one kind of emeraldine state (emeraldine I or emeraldine II) was formed, because the chemical structure of the AT was changed after the coupling reaction with the epoxy group, which has a steric hindrance and positive induction effect on the AT segment, and the possible mechanism is still being investigated. Our CV results for the 5% EGDMA hydrogel with AT segments are different from other reports[51,53] where only one oxidation peak was observed for AT segments, probably because the ureido and amide groups are much stronger electron-withdrawing groups than the $-CH_2-$ group. All these UV spectra and CV curves demonstrated that these conductive hydrogels have good electroactivity.

Electrical Conductivity of the Hydrogels. The electrical conductivities of the hydrogels with different AT contents after doping with the same amount of 1 mol/L HCl were determined using a standard four probe technique, and the results are listed in Table 2. The conductivities of the hydrogels with AT contents from 40 wt % to 10 wt % are between 1.05×10^{-4} and 4.69×10^{-7} S/cm, which is lower than that of AT films. This is because the nonconjugated AC-PLA-PEG-PLA-AC, GMA, and EGDMA components were introduced into the hydrogel network. However, these conductivity values are adequate to transfer bioelectrical signals in vivo, since the microcurrent intensity in the human body is quite low.[54] It was also found that the electrical conductivity increased with increasing AT content in the hydrogels. This is probably because the AT segments in the network allowed better p$-\pi$ stacking of the AT moieties with a higher AT content in the polymer matrix and so facilitate hopping. A broad range of electrical conductivities of these hydrogels was obtained by changing the AT content, which provides wide choices for specific applications.

Table 2. AT Content and Conductivity of the Hydrogels

sample name	AP content by TGA	conductivity (S/cm)
10% AT hydrogel	9.4%	4.69×10^{-7}
20% AT hydrogel	19.1%	4.97×10^{-6}
30% AT hydrogel	30.3%	7.89×10^{-5}
40% AT hydrogel	39.2%	1.05×10^{-4}

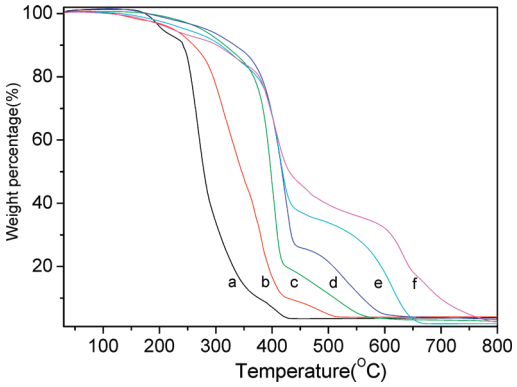

Figure 5. TGA thermograms of (a) AC-PLA-PEG-PLA-AC, (b) AC-PLA-PEG-PLA-AC/GMA after UV irradiation, (c) 10% AT hydrogel, (d) 20% AT hydrogel, (e) 30% AT hydrogel, and (f) 40% AT hydrogel.

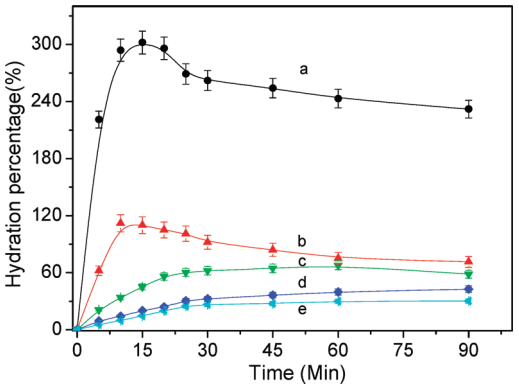

Figure 6. Effect of AT content on the hydration percentage of the hydrogels: (a) AC-PLA-PEG-PLA-AC hydrogel, (b) 10% AT hydrogel, (c) 20% AT hydrogel, (d) 30% AT hydrogel, and (e) 40% AT hydrogel.

Thermal Properties of the Hydrogels. The thermal properties of the macromonomer and hydrogels were studied by TGA, and the TGA curves are shown in Figure 5. AC-PLA-PEG-PLA-AC (curve a) started to lose weight at about 180 °C and was almost totally degraded at 420 °C. Compared with AC-PLA-PEG-PLA-AC, the UV-cross-linked AC-PLA-PEG-PLA-AC/GMA hydrogel has a much higher thermal stability in curve b in Figure 5, because the hydrogel network restricts the motion of the macromolecular chains, which also indicated that the UV-photo-cross-linked reaction has taken place, as demonstrated by FT-IR in Figure 2. In the case of the conductive hydrogels, the degradation was in a two-step process. The first obvious weight

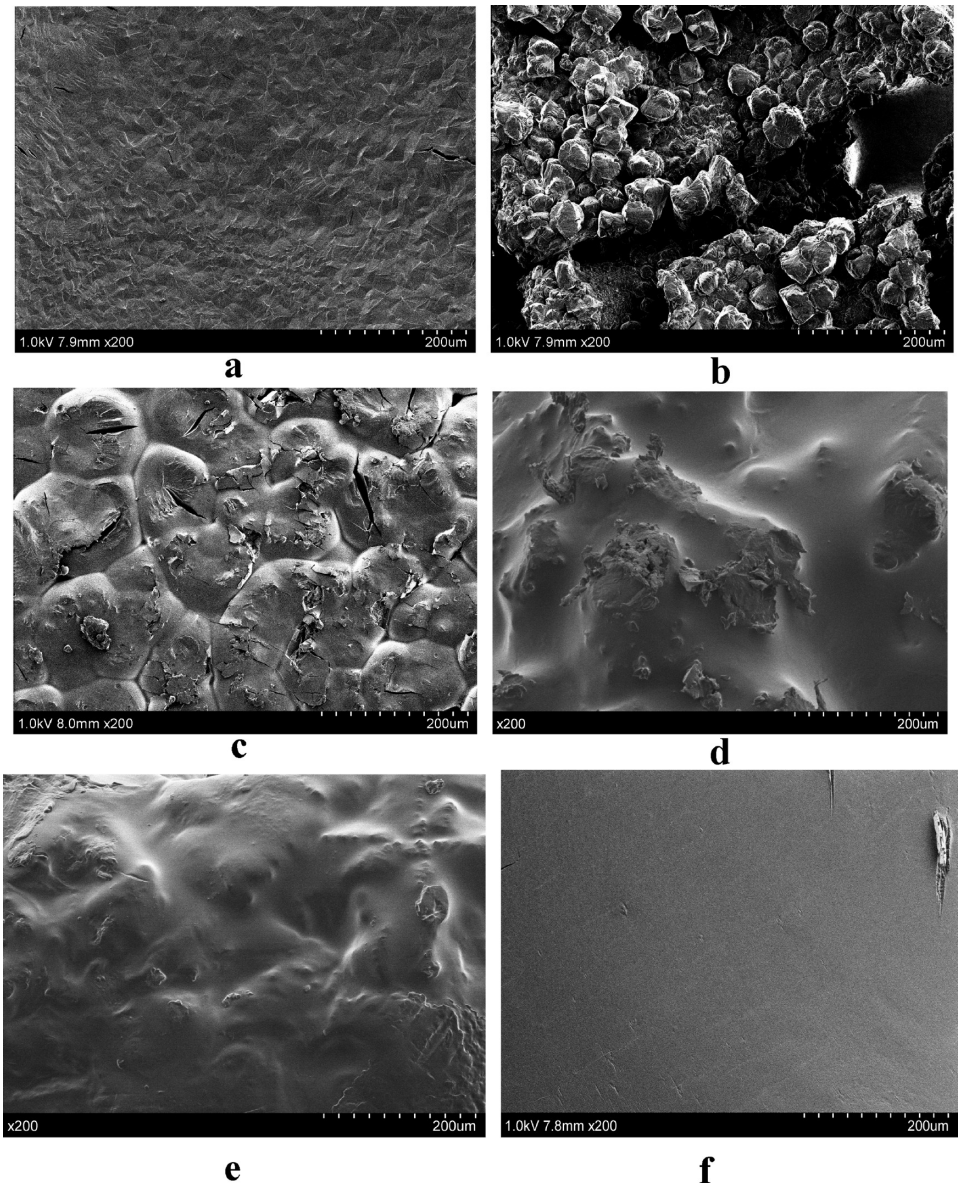

Figure 7. SEM images of the hydrogels: (a) surface of AC-PLA-PEG-PLA-AC/GMA, (b) cross-section of AC-PLA-PEG-PLA-AC/GMA, (c) 10% AT hydrogel, (d) 20% AT hydrogel, (e) 30% AT hydrogel, and (f) 40% AT hydrogel.

loss occurred between 100 °C and 420−455 °C for hydrogels with different AT contents. From 100 °C, the slight weight loss of the conductive hydrogel is ascribed to the loss of solvent and water trapped in the hydrogel network. The AC-PLA-PEG-PLA-AC, GMA, and EGDMA components completely degrade when the temperature rose to 420−455 °C. The second evident weight loss of the hydrogels from 420 to 455 °C is assigned to the degradation of the AT segments linked to the hydrogel network. The starting temperatures for the degradation of 10% AT hydrogel, 20% AT hydrogel, 30% AT hydrogel, and 40% AT hydrogel were 420 °C, 440 °C, 450 °C, and 455 °C, respectively, indicating that the thermal stability of the hydrogels increased with increasing AT content in the hydrogel, probably due to the greater thermal stability of the AT segments. The AT contents in the hydrogels were calculated using the TGA curves by taking the residual weight of 10% AT hydrogel, 20% AT hydrogel, 30% AT hydrogel, and 40% AT hydrogel at 420 °C, 440 °C, 450 °C, and 455 °C and subtracting the weight of cross-linked AC-PLA-PEG-PLA-AC hydrogel at the same temperature, and the results are listed in Table 2. It was found that the data obtained from TGA curves were close to the theoretical values, which also confirms the successful synthesis of the hydrogels.

Swelling of the Hydrogels. The swelling behavior is important for the application of the hydrogels. The HP of the hydrogels was dependent on the AT content in the hydrogels, the cross-linking degree, and the pH value of the solution. Therefore, the HP can be tuned to meet the requirements of a specific application. Figure 6 shows the effect of AT content on the HP of these hydrogels. It was found that the AC-PLA-PEG-PLA-AC hydrogel swells most rapidly and has the highest HP and that the HP of the other hydrogels decreased with increasing AT content in the hydrogel. This is because the AC-PLA-PEG-PLA-AC is more hydrophilic than the AT segments. The swelling behavior

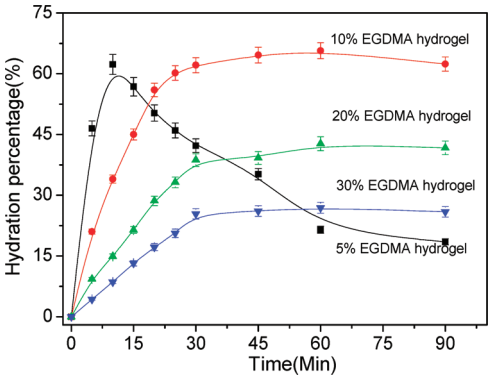

Figure 8. Effect of EGDMA content on the hydration percentage of the hydrogels.

of the hydrogels can also be explained in term of their morphology. Figure 7 shows the SEM of these hydrogels with different AT contents, and it is evident that the AC-PLA-PEG-PLA-AC hydrogel has a rough and condensed surface, although there are plenty of particles inside the hydrogel, as observed in the cross-section of the hydrogel (Figure 7 b). Water molecules can easily penetrate the free space between the particles and are absorbed by the hydrogel. This is why the AC-PLA-PEG-PLA-AC hydrogel reached its maximum HP (about 300%) most rapidly. The hydrogel then cracked into small pieces due to its internal particle structure, and it was difficult to take all the pieces from the water to be weighed; thus, the HP of the AC-PLA-PEG-PLA-AC/GMA hydrogel apparently decreases. From Figure 7c−f, it can be seen that the AT was distributed evenly in the hydrogel matrix and that the surface became increasingly smooth with increasing AT content. It is difficult for the water molecules to penetrate though the smooth surface and into the hydrogels, and the swelling rate of these hydrogels thus decreases with increasing AT content in the hydrogels.

It is known that cross-linking agents have significant effects on the HP of the hydrogels. We added different EGDMA amounts to tune the HPs of the hydrogels, and the results are shown in Figure 8. We found that the HP of 5% EGDMA hydrogels reached about 60 in 10 min and then decreased sharply. This is probably because the water can penetrate into the hydrogel easily with lower cross-linking concentration of the hydrogel; however, the hydrogel partially dissolved because of the low cross-linked density in the network. The 5% EGDMA hydrogels fractured into small pieces, and it was quite hard to take them out from the water to be weighed. These two reasons lead to a decrease in HP of the 5% EGDMA hydrogels. With EGDMA content increasing from 10% to 30%, the HP of the hydrogels decreased. The hydrogels swell more slowly with increasing content of EGDMA, but all the hydrogels reached swelling equilibrium after about 30 min. Sol fraction of the hydrogel describes the fraction of the polymer which is not included in the cross-linked network. The sol fraction of 5% EGDMA hydrogels is about 4%, and the sol fractions of the 10% EGDMA hydrogel, 20% EGDMA hydrogel, and 30% EGDMA hydrogel system after swelling 90 min are around 0.1%, which means the extractables in the hydrogels are quite limited.

The pH of the body fluids varies; thus, it is necessary to study the effect of the pH of the surrounding environment on the HP of the hydrogels for in vivo applications, and the swelling of the hydrogels in solution at pH 2.1 and 7.4 is shown in Figure 9.

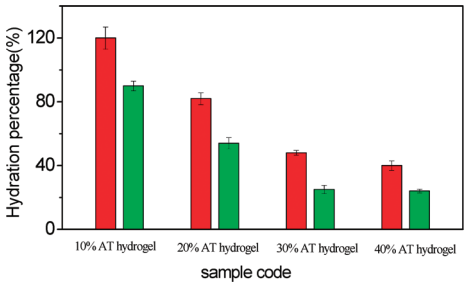

Figure 9. Effect of pH on the hydration percentage of hydrogels: red, pH = 2.1; green, pH = 7.4.

The HP of the hydrogels is greater at pH 2.1 than at pH 7.4. This is probably because in an acidic medium (pH 2.1) the AT segment is doped by the acid, which is associated with hydrated counteranions that serve to maintain charge neutrality of the protonated AT moiety.

CONCLUSIONS

A simple and elegant synthesis route to obtain degradable and electrically conductive hydrogels (DECHs) has been presented. A series of DECHs based on acrylated poly(D,L-lactide)−poly(ethylene glycol)−poly(D,L-lactide) macromer (AC-PLA-PEG-PLA-AC) and aniline tetramer (AT) have been synthesized and characterized by the facile coupling reaction between the epoxy group of glycidyl methacrylate (GMA) in the network and the amino group of AT. The electroactivity of these hydrogels was confirmed by cyclic voltammetry, which showed two pairs of reduction−oxidation peaks, and the conductivity varied between 1.05×10^{-4} and 4.69×10^{-7} S/cm. In addition, it was possible to tune the hydration percentages from 302% to 18.5% by changing the cross-linking density or the pH. The possibility of tuning both the conductivity and the hydration percentage makes it possible to meet the demands of many specific applications. These hydrogels which combine biodegradability from the polyester segment and electroactivity from conducting polymers will greatly expand the application field of conducting hydrogels toward new fields. They are promising candidates for the third generation biomaterials and will open up a range of exciting potential applications in the biomedical field, including drug delivery and tissue regeneration.

ASSOCIATED CONTENT

Supporting Information. ^{1}H NMR and ^{13}C NMR spectra of AC-PLA-PEG-PLA-AC macromer (PDF). This material is available free of charge via the Internet at http://pubs.acs.org.

AUTHOR INFORMATION

Corresponding Author

*Tel.:+46-8-790 8274. Fax: +46-8-20 84 77. E-mail: aila@polymer.kth.se.

ACKNOWLEDGMENT

The authors thank the Swedish Research Council (Grant No. 2008-5538), the China Scholarship Council (CSC), and The Royal Institute of Technology (KTH) for financial support for this work.

REFERENCES

(1) Hench, L. L.; Polak, J. M. *Science* **2002**, *295*, 1014.
(2) Wong, J. Y.; Langer, R.; Ingber, D. E. *Proc. Natl. Acad. Sci. U.S.A.* **1994**, *91*, 3201–3204.
(3) Yousaf, M. N.; Houseman, B. T.; Mrksich, M. *Angew. Chem., Int. Ed.* **2001**, *40*, 1093.
(4) Quigley, A. F.; Razal, J. M.; Thompson, B. C.; Moulton, S. E.; Kita, M.; Kennedy, E. L.; Clark, G. M.; Wallace, G. G.; Kapsa, R. M. I. *Adv. Mater.* **2009**, *21*, 4393.
(5) Luo, W.; Chan, E. W. L.; Yousaf, M. N. *J. Am. Chem. Soc.* **2010**, *132*, 2614–2621.
(6) Gabriel, S.; Cecius, M.; Fleury-Frenette, K.; Cossement, D.; Hecq, M.; Ruth, N.; Jerome, R.; Jerome, C. *Chem. Mater.* **2007**, *19*, 2364–2371.
(7) Guimard, N. K.; Gomez, N.; Schmidt, C. E. *Prog. Polym. Sci.* **2007**, *32*, 876–921.
(8) Gopalan, A. I.; Lee, K. P.; Ragupathy, D.; Lee, S. H.; Lee, J. W. *Biomaterials* **2009**, *30*, 5999–6005.
(9) Zelikin, A. N.; Lynn, D. M.; Farhadi, J.; Martin, I.; Shastri, V.; Langer, R. *Angew. Chem., Int. Ed.* **2002**, *41*, 141–144.
(10) Rivers, T. J.; Hudson, T. W.; Schmidt, C. E. *Adv. Funct. Mater.* **2002**, *12*, 33–37.
(11) Huang, L. H.; Hu, J.; Lang, L.; Wang, X.; Zhang, P. B.; Jing, X. B.; Wang, X. H.; Chen, X. S.; Lelkes, P. I.; MacDiarmid, A. G.; Wei, Y. *Biomaterials* **2007**, *28*, 1741–1751.
(12) Guo, B. L.; Finne-Wistrand, A.; Albertsson, A. C. *Biomacromolecules* **2010**, *11*, 855–863.
(13) Guo, B. L.; Finne-Wistrand, A.; Albertsson, A. C. *Macromolecules* **2010**, *43*, 4472–4480.
(14) Lee, K. Y.; Mooney, D. J. *Chem. Rev.* **2001**, *101*, 1869–1879.
(15) Peppas, N. A.; Hilt, J. Z.; Khademhosseini, A.; Langer, R. *Adv. Mater.* **2006**, *18*, 1345–1360.
(16) Voepel, J.; Edlund, U.; Albertsson, A. C. *J. Polym. Sci., Part A: Polym. Chem.* **2009**, *47*, 3595–3606.
(17) Roos, A. A.; Edlund, U.; Sjoberg, J.; Albertsson, A. C.; Stalbrand, H. *Biomacromolecules* **2008**, *9*, 2104–2110.
(18) Ryner, M.; Valdre, A.; Albertsson, A. C. *J. Polym. Sci., Part A: Polym. Chem.* **2002**, *40*, 2049–2054.
(19) Malberg, S.; Plikk, P.; Finne-Wistrand, A.; Albertsson, A. C. *Chem. Mater.* **2010**, *22*, 3009–3014.
(20) Andreopoulos, F. M.; Deible, C. R.; Stauffer, M. T.; Weber, S. G.; Wagner, W. R.; Beckman, E. J.; Russell, A. J. *J. Am. Chem. Soc.* **1996**, *118*, 6235–6240.
(21) Nguyen, K. T.; West, J. L. *Biomaterials* **2002**, *23*, 4307–4314.
(22) Hiemstra, C.; Zhou, W.; Zhong, Z. Y.; Wouters, M.; Feijen, J. *J. Am. Chem. Soc.* **2007**, *129*, 9918–9926.
(23) Elisseeff, J.; Anseth, K.; Sims, D.; McIntosh, W.; Randolph, M.; Langer, R. *Proc. Natl. Acad. Sci. U.S.A.* **1999**, *96*, 3104–3107.
(24) Jeong, B.; Kim, S. W.; Bae, Y. H. *Adv. Drug Delivery Rev.* **2002**, *54*, 37–51.
(25) Asoh, T. A.; Matsusaki, M.; Kaneko, T.; Akashi, M. *Adv. Mater.* **2008**, *20*, 2080.
(26) Vermonden, T.; Fedorovich, N. E.; van Geemen, D.; Alblas, J.; van Nostrum, C. F.; Dhert, W. J. A.; Hennink, W. E. *Biomacromolecules* **2008**, *9*, 919–926.
(27) Hou, Y.; Matthews, A. R.; Smitherman, A. M.; Bulick, A. S.; Hahn, M. S.; Hou, H.; Han, A.; Grunlan, M. A. *Biomaterials* **2008**, *29*, 3175–3184.
(28) Mellott, M. B.; Searcy, K.; Pishko, M. V. *Biomaterials* **2001**, *22*, 929–941.
(29) Aimetti, A. A.; Machen, A. J.; Anseth, K. S. *Biomaterials* **2009**, *30*, 6048–6054.
(30) Hoshikawa, A.; Nakayama, Y.; Matsuda, T.; Oda, H.; Nakamura, K.; Mabuchi, K. *Tissue Eng.* **2006**, *12*, 2333–2341.
(31) Underhill, G. H.; Chen, A. A.; Albrecht, D. R.; Bhatia, S. N. *Biomaterials* **2007**, *28*, 256–270.
(32) Guiseppi-Elie, A; Wilson, A. M. *Polym. Prepr.* **1997**, *38*, 608.
(33) Guiseppi-Elie, A. *Biomaterials* **2010**, *31*, 2701–2716.
(34) Small, C. J.; Too, C. O.; Wallace, G. G. *Polym. Gels Networks* **1997**, *5*, 251–265.
(35) Ferris, C. J.; Panhuis, M. I. H. *Soft Matter* **2009**, *5*, 3430–3437.
(36) Justin, G.; Guiseppi-Elie, A. *Biomacromolecules* **2009**, *10*, 2539–2549.
(37) Brahim, S.; Guiseppi-Elie, A. *Electroanalysis* **2005**, *17*, 556–570.
(38) Miller, L. L.; Zinger, B.; Zhou, Q. X. *J. Am. Chem. Soc.* **1987**, *109*, 2267–2272.
(39) Miller, L. L. *Mol. Cryst. Liq. Cryst.* **1988**, *160*, 297–301.
(40) Brahim, S.; Narinesingh, D.; Guiseppi-Elie, A. *Biosens. Bioelectron.* **2002**, *17*, 53–59.
(41) Rozalska, I.; Kulyk, P.; Kulszewicz-Bajer, I. *New J. Chem.* **2004**, *28*, 1235–1243.
(42) Sun, Z. C.; Kuang, L.; Jing, X. B.; Wang, X. H.; Li, J.; Wang, F. S. *Chem. J. Chinese U* **2002**, *23*, 496–499.
(43) Lee, W. C.; Li, Y. C.; Chu, I. M. *Macromol. Biosci.* **2006**, *6*, 846–854.
(44) Chen, Y. J.; Kang, E. T.; Neoh, K. G.; Tan, K. L. *Macromolecules* **2001**, *34*, 3133–3141.
(45) Chen, Y. J.; Kang, E. T.; Neoh, K. G.; Tan, K. L. *J. Phys. Chem. B* **2000**, *104*, 9171–9178.
(46) Jana, T.; Nandi, A. K. *Langmuir* **2001**, *17*, 5768–5774.
(47) Marcasuzaa, P.; Reynaud, S.; Ehrenfeld, F.; Khoukh, A.; Desbrieres, J. *Biomacromolecules* **2010**, *11*, 1684–1691.
(48) Quick, D. J.; Anseth, K. S. *J. Controlled Release* **2004**, *96*, 341–351.
(49) Nuttelman, C. R.; Rice, M. A.; Rydholm, A. E.; Salinas, C. N.; Shah, D. N.; Anseth, K. S. *Prog. Polym. Sci.* **2008**, *33*, 167–179.
(50) Parsa, A.; Ab Ghani, S. *Electrochim. Acta* **2009**, *54*, 2856–2860.
(51) Chen, R.; Benicewicz, B. C. *Macromolecules* **2003**, *36*, 6333–6339.
(52) Wang, H. F.; Guo, P.; Han, Y. C. *Macromol. Rapid Commun.* **2006**, *27*, 63–68.
(53) Yang, Z. F.; Wang, X. T.; Yang, Y. K.; Liao, Y. G.; Wei, Y.; Xie, X. L. *Langmuir* **2010**, *26*, 9386–9392.
(54) Niple, J. C.; Daigle, J. P.; Zaffanella, L. E.; Sullivan, T.; Kavet, R. *Bioelectromagnetics* **2004**, *25*, 369–373.